Publisher: Engineering College, Al Muthanna University

Open Access

DOI:10.52113/3/eng/mjet/2025-13-02-/79-89, Vol. (13), Issue (2), 2025

Muthanna Journal of Engineering and Technology
MJET

Submitted 15 May 2025, Accepted 20 June 2025, Published online 18 July 2025

Performance Evaluation of Prestress Bridge Using Field Monitoring and CSI Bridge Modelling

Zinah Ayad Jabbar [1a], Hussein Yousif Aziz [2b]

[a] *civil engineering department, Al-Muthanna University, Al-Samawahh, Iraq*
[b] *civil engineering department, Al-Muthanna University, Al-Samawahh, Iraq*
**Corresponding author: husseinyousifaziz@mu.edu.iq*

Abstract

Brides are important to any transport system network connecting roads and villages with cities. Many Iraqi bridges remain in poor condition even after inspection and confirmation that they are of acceptable standards due to the role played by various risk factors, including traffic volume and insufficient capacity. Effects of changed patterns of operational loads, slack, deterioration, and other man-made effects on bridge construction cause its degeneration. The primary purpose of this research was to determine the structural condition of the superstructure of the Barboty bridge and any associated damage, if any, utilizing strain, displacement sensors, and CSI Bridge software which is employed to generate the finite element model of the bridge superstructure. The difference between the experimental and analysis results was about 10.60 %, representing good agreement. Maximum deflections in both static and dynamic conditions were found to be within the allowable limit (L/800) as stated in the AASHTO code. Deflections, distribution factors, modal curvature, and rating factor classification were extracted. The distribution factor ratio provided a conservative outcome that was approximately 80% below the AASHTO requirements. All other parameters were found under AASHTO specifications, and no abnormal condition was observed.

Keywords: *Bridge, Structural Health Monitoring, Distribution factor, Rating factor, Modal Curvatures*

1. Introduction

Any nation requires bridges as basic infrastructure elements to be essential transport links between road systems and rural and urban areas. These structures experience different operational loads, and exposure to events and human factors that create multiple deterioration mechanisms, such as cyclic loads, cause their performance to decrease with time. Assessing structural conditions becomes imperative to determine necessary actions between demolition or maintenance since operational loads during the design phase typically do not match actual field conditions. In this context, constantly monitoring the performance of structures is referred to as the term Structural Health Monitoring (SHM). According to Olaszek et al. [1], they used diagnostic tests to assess conditions. assessing reinforced, prestressed, and steel bridges are also included in their responsibilities. Considered into the requirements of bridge construction and bridge inspections when they used test loads. The agreement is considered acceptable when the difference between the site measurement values and the analytical values is within ±10% and ±15% for precast concrete, steel bridges, reinforced concrete and composite bridges, respectively. Kaloop et al. [2], tested a pre-stressed concrete and steel bridges under conducted diagnostic testing, and their structural reaction was examined using loading data from previously. The AASHTO standards' design and construction requirements were considered along to assess the bridges' real performance and contrast it with the behavior that the models anticipated. A thorough examination of the loading conditions and the physical characteristics of the structural components was also included in the investigation in order determine if the bridges conformed with the criteria and evaluate their long-term structural effectiveness. In addition to the use of field tests and analytical investigations for decision making, a generic framework for describing structures including bridge testing—is presented in detail [3]. A particular bridge may be tested to

This is an open access article under the terms of the Creative Commons Attribution License, which permits use, distribution and reproduction in any medium, provided the original work is properly cited. © 2025 The Authors

identify important issues, and sometimes, a sample of typical bridges can be assessed to address issues related to a similar bridge [4]. To conduct a rapid experimental test on a group of reinforced concrete bridges, the researchers proposed a method for determining moment slope factors for single-span girder bridges [5]. They demonstrated that the new approach can reasonably predict the live load compared to the standard girder analysis provided in the AASHTO code (2017) [6]. The results of load rating factors for a fully fabricated bridge were obtained through three methods by using the LRFR approach with experimental strains, standards, and finite element methods [7]. The evaluation process helps identify damage and approve precisely maintenance solutions that guarantee safety and operational longevity within civil engineering domains. In recent times, SHM technologies have drawn rising interest because they help address various aging infrastructure challenges while lowering maintenance expenses, extending facility lifespans, and diminishing direct human maintenance needs [8]. The researchers [9-12] reviewed bridge behavior during standard loads and evaluated the bridges' validity to carry such loads under investigations that inspected I-girder bridges for health conditions. Static tests with various truck loads allowed investigators to calculate the distribution factor (DF) and load rating (RF) factors and perform bridge deflection checks. Prestressing systems can be defined as initially loading a structure before it is based to operational loads, aiming to enhance their resistance and improve their performance. These systems are divided into two main types: prestressing with pretension and prestressing with post-tensioning. These systems use high-strength steel tendons, effectively strengthening concrete elements and improving their structural behavior [13, 14]. The researchers established an experimental method to determine the moment DFs for single-span beam bridges as part of rapid population testing [5]. Non-destructive testing can be used to calculate the compressive strength of concrete [15]. A static load test was conducted on the bridge to extract displacement and distribution factor (DF) values. The results showed that all these values were approximately 90% lower than specified in the AASHTO specifications, indicating the conservative structural behavior of the bridge and its ability to safely withstand loads that exceed the approved design requirements [16]. The researchers found that their new approach accurately predicted live load results, which matched the standard girder modeling method specified in AASHTO, 2017 [6]. In addition, very few studies addressed the behaviors of bridge girders for structures behaviors. The curvature model was used to detect damage to the bridge [17]. In addition, the curvature modal was used to estimate the damage to simple reinforced concrete girders, and the results demonstrated its applicability for detecting minor damage [18]. Finally, the primary objective of this research is to assess the health of the bridge's superstructure. Furthermore, the actual field test and finite element method will be validated, and various bridge parameters will be determined using load test data.

2. Bridge description

The Barboty Bridge is one of the bridges over the Euphrates River, located in the AL-Muthanna governorate in Iraq. It connects the city's neighborhoods and provides a northern entrance to Samawah. The composite bridge consists of five spans, the length of which is 154 m long. The middle span is steel 54 m length, and the remaining four spans are prestressed concrete 25 m length for each. as shown in Figure 1. The bridge's width is 16 m, consisting of a four-traffic lane with 13.57 m wide, each lane equal is 3.75 m, and the walkway is 1.25 m wide on the left and right sides of the carriageway. The concrete deck thickness is 0.23 m, and the asphalt surface is 0.06 m, with a slope of 2%. The dimension of the concrete girder is (1.20*0.60) m, with prestress concrete girders at 1.508 m center to center. The dimensions of the steel girder are (2*0.60) m in dimensions, with 2.715 m in diaphragm crossing at each steel section. The instrumentation was selected during the load test to provide maximum information about the behavior of the bridge girders. The sensor locations were chosen at the critical mid-span location. Since the bridge cannot be closed to traffic, it was decided to use only one span for this study. Mounting sensors at the mid-span poses significant challenges due to its location above the waterline. Therefore, the study decided to focus on the second span of the concrete girder. The three end girders on the left were used to represent the lane used for truck traffic. The sensors were installed below the girders by removing the strain adhesive, sanding the girders to remove any roughness, and then securely fastening them. A displacement sensor was securely attached to the 75 cm long steel section and elevated below the girders by erecting a 6 m-long metal scaffold, installing the sensors, and connecting them to a user data collection device. Each girder is equipped with a displacement and strain sensor and an accelerometer, making the monitoring process part of a building health

monitoring system that continuously and directly monitors the condition of buildings, detects early structural changes, and examines the bridge's response under loads. Figure 2 shows the sensors during installation.

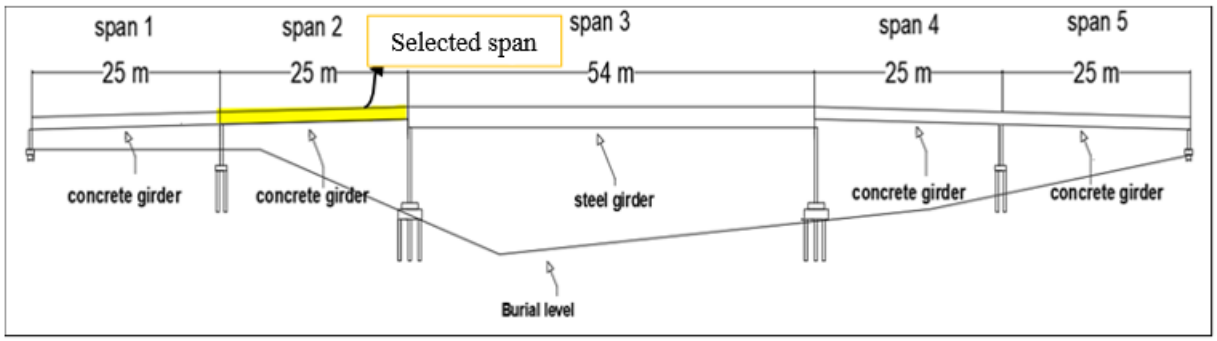

Fig. 1: Cross section of the bridge

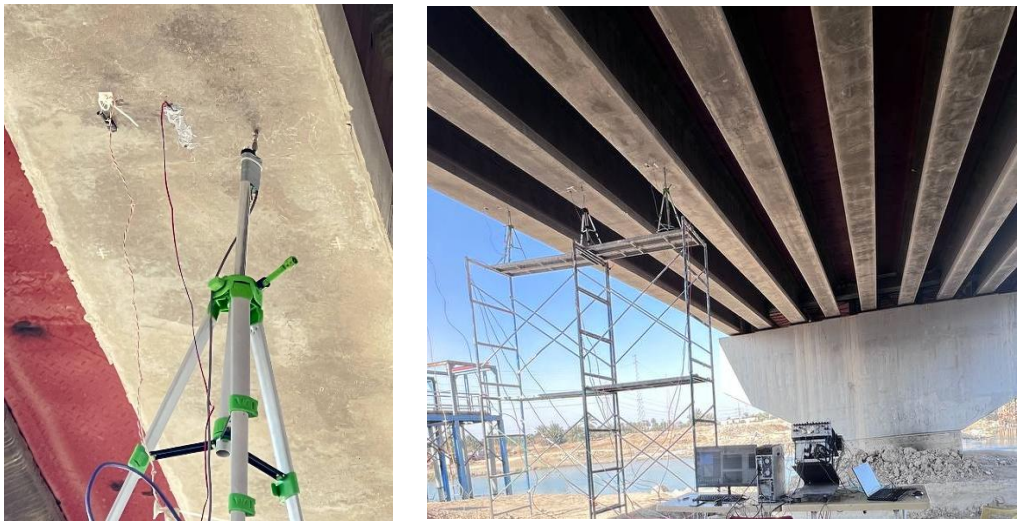

Fig. 2: Installing of sensors

3. Bridge modeling

Only one span, the second span with prestressed girders, was selected for the practical application. The three sensors were used for modeling and analyzing the bridge superstructure LVDT, strain gauge, and accelerometer using simple-support boundary conditions using the finite element software CSI Bridge V25. CSI Bridge is one of the most versatile and productive bridge modeling, analysis, and design software. Using a compressive strength of 36 MPa, a modulus of elasticity of 28200 MPa, a unit weight of 23.5 kN/m³, and a concrete properties ratio of 0.2, the bridge was modeled and analyzed based on the measured data. The FE analysis of the bridge employed beam and shell elements for both prestress of concrete and deck slap. Figure 3 shows the FE model of girders and decks built with elements. The assessment included tendon elements, which represented the prestressing effect. The bridge's calculation report and project drawings provided these specifications. All intended elements of the FEM made it through bridge drawings. According to the experimental field test, the bridge received updates, which provided modal characteristics that achieved this goal strain and displacement results [19, 20].

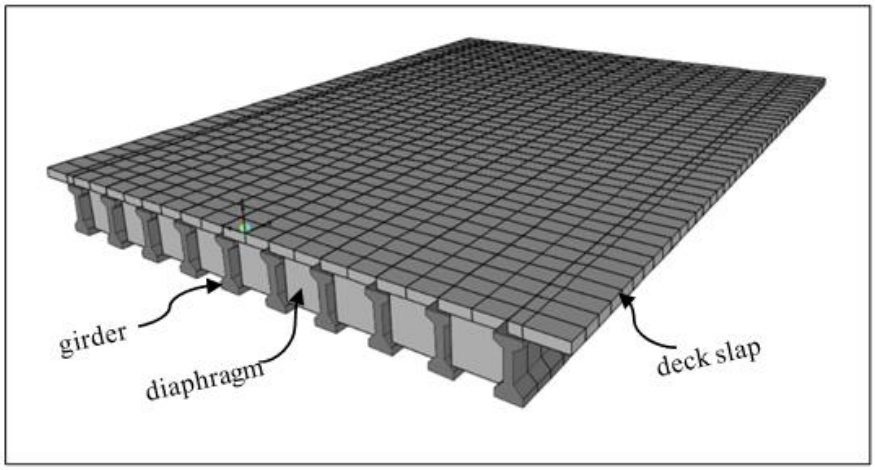

Fig. 3: FE model span of bridge

4. Field investigation

The response of bridge girders to vehicle loads becomes apparent through properly analyzed load test results. The development of complex behaviors allows simple observational records to facilitate meaningful performance assessments between different cases. The LVDT and strain sensors were installed under three girders of bridge, connected to a data actuation system to store and record data. With truck a known weight of 70% of the design load [10], The Mercedes-Benz Actros 8×4 dump truck was used in this study with dump load is 33 m3. The truck was loaded with washed sand weighing 1800 kg /m3 as shown in Figure 4. The test truck stopped in the center of the span above the sensors to record the maximum response. It then traveled along the specified path at various speeds. An analysis was attempted to divide girder behavior from other participating bridge structures while assessing load test outcomes. Research has narrowed its investigation into girder reactions since it is expected to experience the most substantial effects from passing vehicles to ensure the safety of utility crews and vehicles during inspections. The research examines recorded displacements and strains due to the subsequent analysis involves these measurements.

Fig. 4: truck test

5. Results and discussions

5.1. Field test results

Table 1 shows the relationship between the single-truck bridge girders with displacement and strain resulting from field tests from static tests. The results indicate a good distribution of the girders, with the maximum value for girder G2 directly under the load test. Table 2 shows data from a dynamic test of a prestressed bridge, where displacement and strain were measured at three points (G1, G2, G3) on the bridge when vehicles passed at different speeds (20, 40, 60 km/h). The results were obtained when the truck passed the specified path for the sensors under the three girders. The displacement increases with increasing speed up to 40 km/h, then begins to decrease at 60 km/h, indicating that the interaction between the bridge and the

truck may be more influential at a certain speed or due to noise affecting the results, after which dynamic effects begin to reduce the displacement due to inertial forces. At 40 km/h, all girders showed an increase in strain, with the highest value at G2 (49 με).

Table 1: Experiment result of static load test

Displacement (mm)			Strain (με)		
G1	G2	G3	G1	G2	G3
3.47	3.62	3	52.80	53.80	42.50

Table 2: Experiment result of displacement and strain girders under dynamic loads

Speed km/h	Displacement (mm)			Strain (με)		
	G1	G2	G3	G1	G2	G3
20	3.03	3.47	2.14	41	48.30	32.3
40	3.13	3.46	2.53	48.18	49	44.28
60	2.91	3	2.51	46.52	48.22	43.34

The results obtained from the truck passing test appear lower compared to static load test outcomes. The significant difference between girders, as shown in Table 3, is that G1, G2, and G3 result in substantial displacement measurements of 20.17 %, 5.80 %, and 28.60 %, respectively. It indicates a limited effect of dynamic loads on this type of bridge. The linear extrapolation of a single truck passing displacement development could explain these results since the real measurements possibly contain nonlinear elements. A possible non-linear relationship exists between the additional displacement and increased load capacity during analysis. The same case showed that the destructive test on a PC girder bridge displayed an equivalent nonlinearity effect when applying maximum pregnancy from zero load [21].

Table 3: Different displacement between static and dynamic test, unit in (mm)

Girders	Disp. Static	Disp. 20 km/h	Disp. 40 km/h	Disp. 60 km/h	Different from static results %		
G1	3.47	3.03	3.13	2.91	12.68	9.79	20.17
G2	3.62	3.47	3.46	3	4.14	4.41	5.80
G3	3	2.14	2.53	2.51	28.60	15.67	8.67

5.2. Numerical analysis and experimental for static results

The same truck was calculated to represent the same field conditions on the real bridge. Figure 5 shows the data obtained for the static test. The vertical displacement and strain were obtained at mid-span when the truck was stationary. During fieldwork, the truck stopped in the middle of the space and remained stopped for more than one minute when the displacement and strain were constant at 3.62 mm and 53.80 με. The same field conditions were calibrated in the CSI software, and the maximum value of displacement at the middle of the span girder was obtained as 3.40 mm; as for the strain, three points were taken for calibration, one-third of the span, in the middle, and two-thirds of the span. The maximum value in the mid-span was obtained at 48 με.

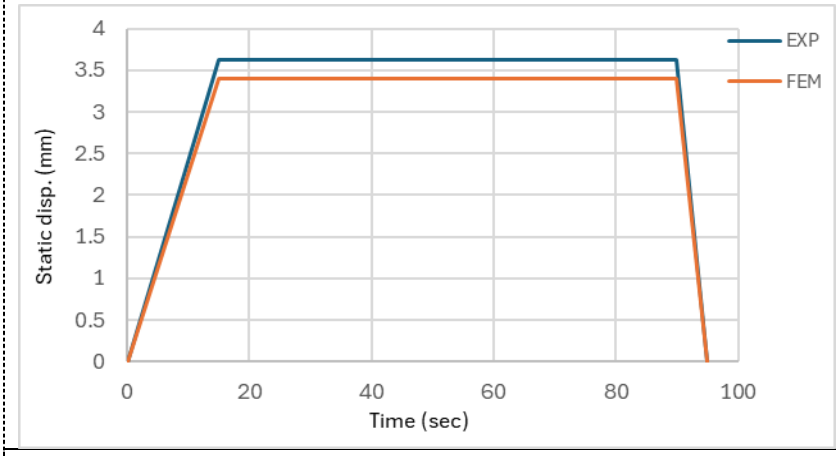

(a)

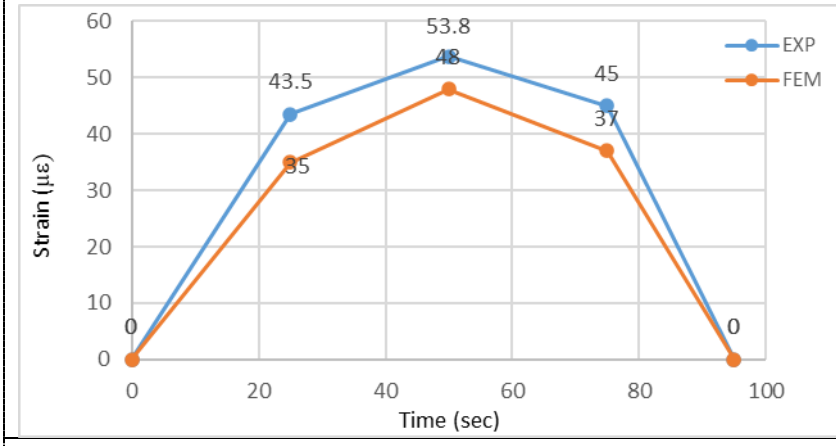

(b)

Fig. 5: Experimental and model data for a static test, (a) displacement, (b) strain

5.3. Numerical dynamic analysis results

FEM analysis focused on girder G2, located below the specified lane, as it was the primary location for assessing the consistency of simulation results with measured experimental data. Specific locations were chosen to match the installation locations of the strain gauges and displacement measuring used in the field experiments. Experimentally measured deflection values were directly compared with the values generated by the model. To calculate strains at the bottom of the prestressed girder, the results of the force analysis generated by the FE model were used, combining the axial force and the resulting moment to determine the stress at the base of the frame element. The strain was calculated by dividing stress by the elasticity of modulus to verify the load test results. Figure 6 shows the comparison and correlation for displacement for all dynamic cases 20 km/h, 40km/h, and 60 km/h, respectively. The correlation is within 0.989 of the actual deviations for the first case. It is also noted that the coefficient of correlation is 0.974 for the second case, indicating an ideal correlation between the FEM and the load test. As for the third case, the correlation coefficient is 0.967, indicating a good correlation value for all cases within ±15%. Therefore, it was decided to consider only the 40 km/h strain condition, as shown in Figure 7. Strain calculations at three points on the girder show that both curves have consistent dynamic behavior starting from zero, reaching a peak, and then gradually decreasing, indicating that the effect of the dynamic load has passed.

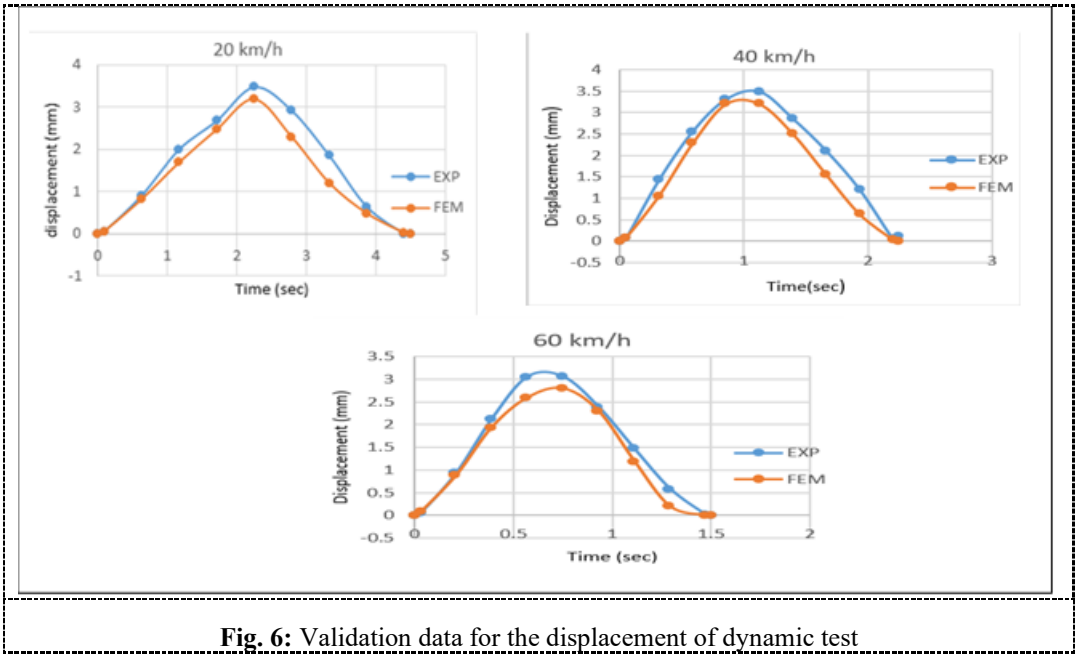

Fig. 6: Validation data for the displacement of dynamic test

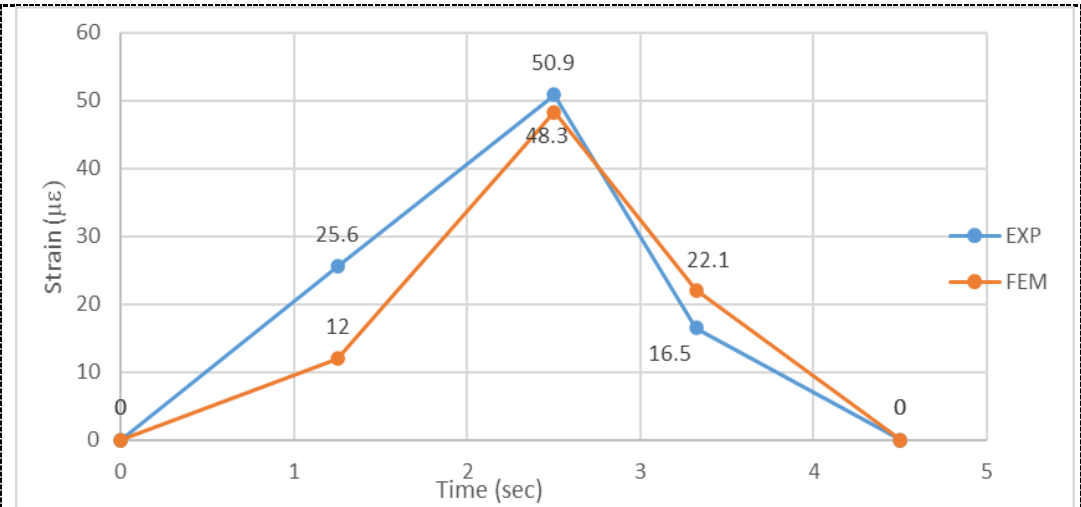

Fig. 7: Validation data for the strain of dynamic test

5.4. Modes shapes

For the identification of shape mode, CSI Bridge software was employed to conduct the modular analysis of calibrated FEM. Shapes mode for concrete spanning was detected. The table lists the values of the natural dynamic frequency with the typical shape of the bridge structure. Figure 8 shows the first six mode shapes of concrete bridge patterns. Monitoring this information and the vehicle response happens efficiently in conditions of low vehicle traffic while tracking stiffness changes or limit state status. The higher the natural frequency of a vibration mode, the more complex its associated modular shape becomes, indicating the bridge's ability to vibrate at higher frequencies. Although these modes typically respond less effectively to low-energy natural dynamic forces, the first mode (Mode 1) is the most dynamically significant, representing the fundamental natural frequency that encompasses the entire bridge's vibration response. This mode is often relied upon in analyzing critical dynamic effects such as heavy vehicle (truck) traffic or seismic activity. In this case, its frequency was 6.39 Hz, indicating a bridge of moderate stiffness. The closeness of the frequencies associated with Modes 3, 4, and 5 suggests the potential for overlapping transverse and/or torsional vibration modes. This may be due to uneven mass distribution or geometric differences in the bridge's dimensions, particularly between width and length. In contrast, the sixth mode, with a frequency of 9.42 Hz, represents a more complex vibration pattern, not typically stimulated by everyday kinetic loads such as vehicle movement, but it is important in the context of analyzing responses resulting from high dynamic loads, such as earthquakes, explosion loads, or severe collisions. Another objective of modal testing is to utilize the collected data to identify any

anomalous structural behaviors that may occur during the passage of the test vehicle. These dynamic responses can be systematically monitored over time to detect any significant variations, which may indicate changes in the structural integrity or the onset of damage.

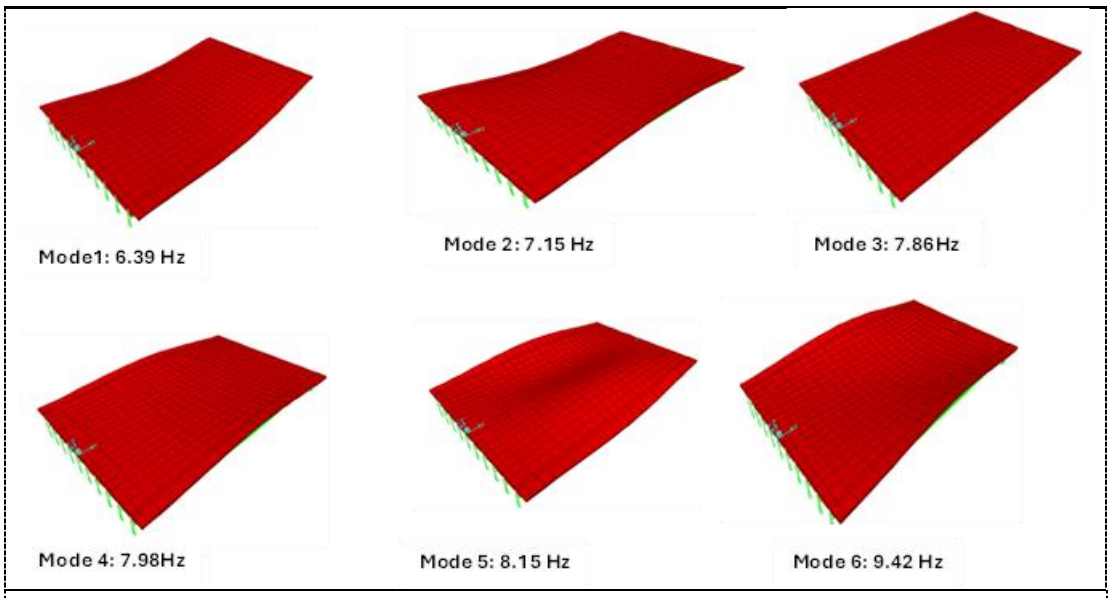

Fig. 8: Six shapes of mode for the bridge

5.5. Distribution Factor

load distribution factor DF is a measure of load transfer across a structure. Generally, bridges are designed to distribute traffic loads across the girders as evenly as possible so that no structural element bears an excessive load. Therefore, when assessing a bridge's load-carrying capacity, particularly for beam-and-slab bridges, the role of code-defined load distribution coefficients is critical in the calculations. For instance, when applying the load to the selected lane, high defensive factors mean poor distribution of the load between the adjacent girders. Therefore, it is assumed that the girders directly subjected to the load will bear a significant portion, making the assessment more conservative. As a result, determining DF is vital in any bridge evaluation. Any change in the condition of a bridge during its operation can significantly affect its distribution characteristics. FEM was updated to calculate the distribution coefficient for the ten beams, Figure (9a) shows the DF of the truck at the static position, and Figure (9b) shows the DF of the truck in the dynamic test. The close values between the displacement and strain distribution enhance the credibility of the numerical model used. The peak values appear in the middle of girders (G1, G2, and G3), then the other girders become almost non-existent at the extreme girders. The maximum value does not exceed 0.3, much less than the 0.5 and 0.55 for interior and exterior girders, respectively, approved in the code AASHTO [6]. The DF of each girder using girder deflections or strain can be determined by Eq. (1) as follows:

$$\mathrm{DFi} = \frac{\alpha i}{\sum_{j=1}^{n} \alpha j} \tag{1}$$

αi and αj represent strains or displacements at the same section, while i and j represent girder numbers depending on the data used.

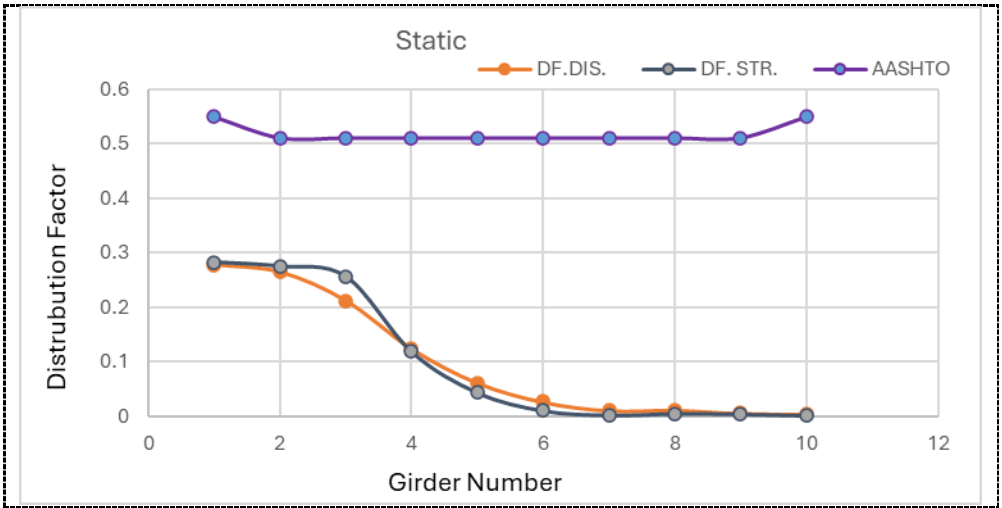

(a)

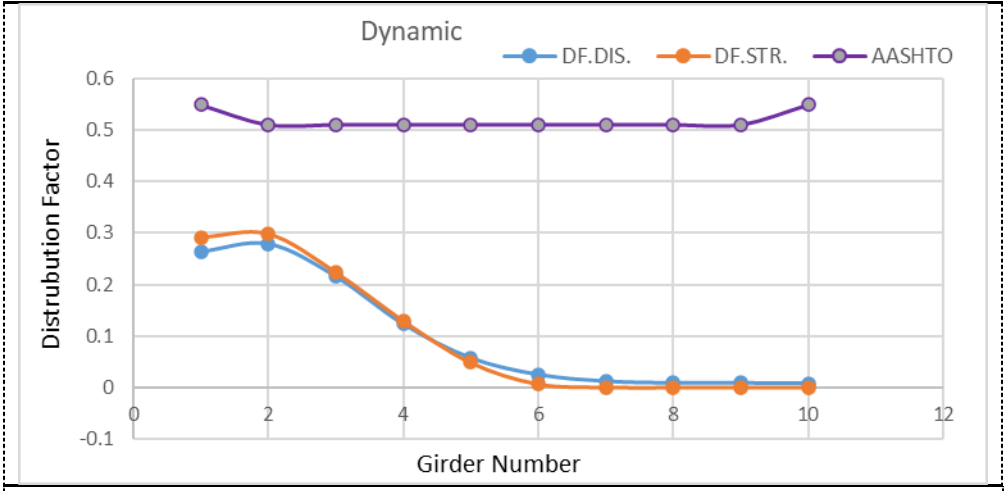

(b)

Fig. 9: Distribution factor for all girders of bridge, (a) static test, (b) dynamic test

5.6. Modal curvatures

Reinders et al.[17] discovered that when evaluating that a structure is damaged, the pattern curvature calculated from strain data is more accurate than the pattern curvature obtained from displacement data. To estimate the pattern curvature, the current study employed data for three girders from the selected truck. Equation (2) represents the formula used to determine the curvature of bridge girders.

$$k = \frac{(\varepsilon_t - \varepsilon_b)}{h} \quad (2)$$

Were, ε_t top strain, ε_b: bottom strain, from validation of finite element method, h: girder height section.

Figure 10 displays the determined curvature values for girders G1, G2, and G3. According to the findings, girder G2 had the greatest curvature under static loading conditions, followed by G1 and G3. This implies that, among the girders under observation, G2 underwent the most flexural deformation, most likely due to its direct location beneath the applied load. This girder's sensitivity to load-induced bending is further supported by the observation that G2 continually maintained the greatest curvature values in all scenarios across dynamic testing conducted at different speeds. These dependable results in both static and dynamic settings indicate that static testing might be a useful technique for assessing flexural behavior. Additionally, the three girders' comparable curvature trends under various load scenarios suggest consistent bending behavior across the bridge span. Given that no significant abnormalities or irregularities were found, this consistency lends credence to the idea that the structure is operating properly under service loads. The bridge's existing structural safety is therefore positively indicated by its acceptable flexural performance [22].

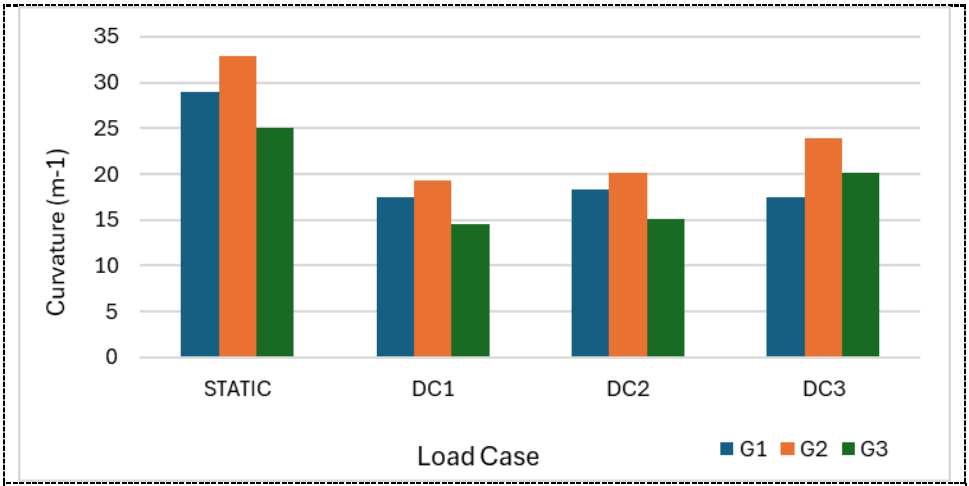

Fig. 10: Curvatures girders under different cases

5.7. Load rating

Bridges are inspected on a regular basis according to a specified schedule in many countries. In China, Japan, and the US, this period is typically around five years [23]. In addition to the regular inspections, bridge operators may arrange for a special inspection within this schedule to check for known or suspected defects, such as those resulting from collisions with vehicles or ships. However, the condition rating systems that are widely used do not usually provide accurate information about the remaining load-bearing capacity of bridges that have suffered significant damage. bridge load capacity is established using the load rating factor, their standard measurement system.

The load rating factor is a bridge capacity measurement that provides permits to heavy trucks and decides bridge load limit postings. The bridge's rating load was determined through a numerical model, as shown in Figure 11. The service rating indicates an external girder load of approximately 1.79 and an internal girder load of approximately 3.21 for a test truck HS20-44. The results were align with [24] Since both load rating factors exceed 1.0, the bridge is considered safe for the truck used in this study according to [1].

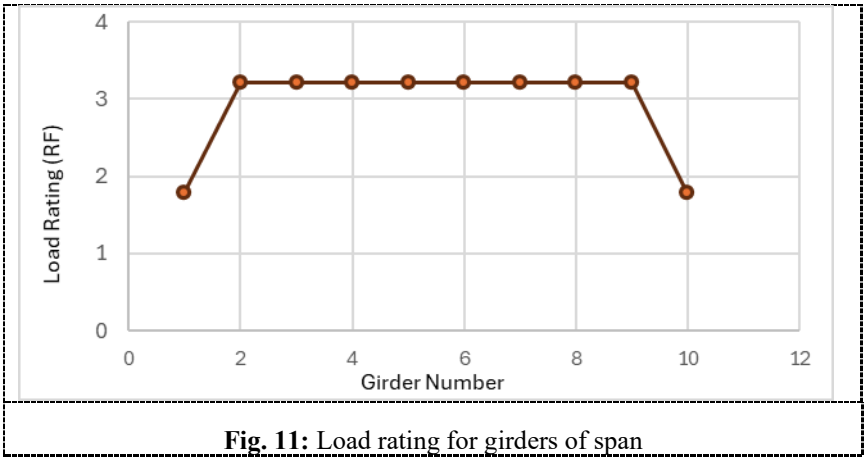

Fig. 11: Load rating for girders of span

6. Conclusion

This study assessed the Barboty Bridge's serviceability under both static and dynamic loads using a short-term, non-destructive structural integrity monitoring method. A test truck was used to apply a single-lane load, which allowed for a highly accurate and reliable calculation of the bridge's load-bearing capacity. Under the bridge girders, displacement and strain sensors have been installed and connected to a gathering system for store data purposes. A field test was conducted to examine the structure of the prestressed concrete girder bridge. The bridge's stress-displacement responses have been studied at various speeds and under static conditions. Three girders were measured, as well as the outcomes for the other girders were calculated using validation from the finite element model (FEM). This study illustrates how the bridge responds to various scenarios, highlighting the impact of several characteristics such load functions, mode shape, deflection limit, and rating factors. It also highlights how these criteria influence technical decisions related to selecting appropriate loads, assessing maintenance needs, determining speed adjustments, and potential structural modifications. Finite element modeling methods were used to compare the field test findings. A comparison of the displacement and strain findings from analytical and experiment tested showed a difference of approximately 10.60%, indicating that the data were in good agreement.

Furthermore, conservative results for both static and dynamic loading conditions were obtained using the distribution factor for live loads. The load determination factor values equal to 0.3 was below the AASHTO-recommended which is 0.55. The load rating factor was found using FEM results for the external girders, the rating factor was 1.79, and for the interior girders, it was 3.21 which shows more than one, means that the bridge girders can safely carry this truck. Furthermore, the finite element model showed an excellent level of concordance with the field test data, allowing analytic derivation of reliable pattern results. As a result, this confirms that the updated finite element model can be dependably used for more advanced analysis of bridge structure. Overall, the research found that bridge condition assessments can be performed quickly and easily without causing any interruptions or traffic closures. Therefore, the framework in this research can be used on other bridges with similar types and characteristics.

References

[1]. Olaszek P, Łagoda M, Casas JRJ. Diagnostic load testing and assessment of existing bridges: examples of application. Engineering. 2014;10(6):834–42.

[2]. Kaloop MR, Kim K-H, Elsharawy M, Zarzoura F, Hu JWJSEI. Performance assessment using a field test of a short-period monitoring system: Tun Bridge case study. Structural Engineering International. 2019;29(4):600–12.

[3]. Çatbaş FN, Kijewski-Correa T, Aktan AEJRASCE. Structural identification of constructed systems. 2013.

[4]. Gokce HB, Catbas FN, Frangopol DM. Evaluation of load rating and system reliability of movable bridge. Transportation Research Record. 2011;2251(1):114–22.

[5]. Catbas FN, Gokce HB, Gul MJBE. Practical approach for estimating distribution factor for load rating: Demonstration on reinforced concrete T-beam bridges. Journal of Bridge Engineering. 2012;17(4):652–61.

[6]. AASHTO. Bridge design specifications. Washington, DC: American Association of State Highway and Transportation Officials; 1998.

[7]. Sanayei M, Reiff AJ, Brenner BR, Imbaro GRJPCF. Load rating of a fully instrumented bridge: Comparison of LRFR approaches. Journal of Performance of Constructed Facilities. 2016;30(2):04015019.

[8]. Lama M, Mandal B, Tamang M. Structural health assessment of the Bagmati Bridge. 2022.

[9]. Liu Z, Freeseman K, Phares BM. Evaluation of the need for negative moment reinforcing in prestressed concrete bridges in the view of service loads. Engineering Structures. 2020;207:110206.

[10]. Kaloop MR, Kim KH, Elbeltagi E, Jin X, Hu JW. Service-life evaluation of existing bridges subjected to static and moving trucks using structural health monitoring system: case study. KSCE Journal of Civil Engineering. 2020;24(5):1593–606.

[11]. Algohi B, Bakht B, Mufti AJCSHM. Long-term study on bearing restraint of a girder bridge. Case Studies in Structural Health Monitoring. 2017;7:45–55.

[12]. El-Sisi AE-DA, El-Husseiny OM, Matar EB, Sallam HE-DM, Salim HAJCSHM. Field-testing and numerical simulation of Vantage steel bridge. Case Studies in Structural Health Monitoring. 2020;10:443–56.

[13]. Jeon J-C, Lee H-H. Development of displacement estimation method of girder bridges using measured strain signal induced by vehicular loads. Engineering Structures. 2019;186:203–15.

[14]. Naser AF, Zonglin WJAE, Sciences. Strengthening of Jiamusi prestressed concrete highway bridge by using external posttensioning technology in China. American Journal of Engineering and Applied Sciences. 2010;5(11):60–9.

[15]. Hussein MO, Mahmoud ASJE. Assessing the aged prestress concrete girder's quality in Al-Rayhanna Bridge using NDT. Journal of Engineering. 2025;2025(1):1096697.

[16]. Athab HF, Aziz HY. Evaluation of safety and operational efficiency using structural health monitoring method. IOP Conf Ser Earth Environ Sci. 2024;1374(1):012087.

[17]. Reynders E, De Roeck G, Gundes Bakir P, Sauvage CJEM. Damage identification on the Tilff Bridge by vibration monitoring using optical fiber strain sensors. Journal of Engineering Mechanics. 2007;133(2):185–93.

[18]. Xue G, Guo X, Dong Z. Study on curvature modal shapes of the damage reinforced concrete beams. In: Computational Structural Engineering: Proceedings of the International Symposium, Shanghai, China, June 22–24, 2009. Springer; 2009. p. 815–21.

[19]. Friswell MI, Mottershead JE. Finite element modelling. Springer; 1995.

[20]. Al-Nasar MKR, Al-Zwainy FMS. Load testing for I-girder type bridge to identify serviceability, load-carrying capacity and dynamic.

[21]. Burdette EG, Goodpasture DW. Test to failure of a prestressed concrete bridge. PCI Journal. 1975;(101).

[22]. Kaloop MR, Kim KH, Elbeltagi E, Jin X, Hu JW. Service-life evaluation of existing bridges subjected to static and moving trucks using structural health monitoring system: Case study. KSCE Journal of Civil Engineering. 2020;24(5):1593–606.

[23]. Mahmood BA, Mohammad KIJES. Finite element analysis for RC deep beams under an eccentric load. Tikrit Journal of Engineering Sciences. 2019;26(1):41–50.

[24]. Dong C, Bas S, Debees M, Alver N, Catbas FN. Bridge load testing for identifying live load distribution, load rating, serviceability and dynamic response. Frontiers in Built Environment. 2020;6.